N85-28904

Cometary Atmospheres:
Modeling the Spatial Distribution of Observed Neutral Radicals

Michael R. Combi

Atmospheric and Environmental Research, Inc.
840 Memorial Drive
Cambridge, MA 02139

June 1985

Annual Report for the Period
June 1, 1984 to May 31, 1985

Prepared for
NASA Headquarters

TECHNICAL REPORT STANDARD TITLE PAGE

1. Report No.	2. Government Accession No.	3. Recipient's Catalog No.

4. Title and Subtitle	5. Report Date
Cometary Atmospheres: Modeling the Spatial Distribution of Observed Neutral Radicals	June 1985
	6. Performing Organization Code
7. Author(s)	8. Performing Organization Report No.
9. Performing Organization Name and Address Atmospheric and Environmental Research, Inc. 840 Memorial Drive Cambridge, MA 02139	10. Work Unit No.
	11. Contract or Grant No. NASW-3950
	13. Type of Report and Period Covered Annual Report 6/1/84 - 5/31/85
12. Sponsoring Agency Name and Address NASA Headquarters Headquarters Contract Division Washington, DC 20546	14. Sponsoring Agency Code
15. Supplementary Notes	

16. Abstract

Progress in the first year of a two-year project on modeling the spatial distributions of cometary radicals is described herein. The Monte Carlo particle-trajectory model has been generalized to include the full time dependencies of initial comet expansion velocities, nucleus vaporization rates, photochemical lifetimes and photon emission rates which enter the problem through the comet's changing heliocentric distance and velocity. The effect of multiple collisions in the transition zone from collisional coupling to true free flow has also been included. Currently available observations of the spatial distributions of the neutral radicals, as well as the latest available photochemical data have been re-evaluated. Preliminary exploratory model results testing the effects of various processes on observable spatial distributions is also discussed in this report.

17. Key Words (Selected by Author(s))	18. Distribution Statement
comets	

19. Security Classif. (of this report)	20. Security Classif. (of this page)	21. No. of Pages	22. Price*
Unclassified	Unclassified		

*For sale by the Clearinghouse for Federal Scientific and Technical Information, Springfield, Virginia 22151.

I. Introduction

This report describes the progress made in the first year of a two-year project which deals with modeling the spatial distributions of observed cometary radicals.

The primary goals of the research program are the inclusion and evaluation of the following processes which are usually neglected in modeling cometary atmospheres: (1) dependence on heliocentric distance of initial comet expansion velocities and nucleus vaporization rates, (2) dependence on heliocentric velocity of photochemical lifetimes and photon emission rates where applicable, (3) the correct isotropic ejection of daughter radicals upon photodissociation of parent molecules, (4) solar radiation pressure, and (5) collisional effects on radical kinematics. The principal results of the modeling effort would be to generate the information necessary to reduce observed radical column abundances to radical production rates for CN, C_2, C_3, and OH. Secondary goals which would naturally follow would be a better quantitative understanding of the physical processes which are important in cometary atmospheres. In all instances model development is constrained by the observed spatial distributions of these radicals already published in the literature, as well as by the best currently available photochemical data. In addition, the same models developed here could also be easily applied to analyze the new observed spatial distributions of cometary radicals.

A fairly large amount of the filter photometric data can be expected to be acquired during the 1985-1986 apparition of Comet P/Halley from the members of the Photometry/Polarimetry network organized under the International Halley Watch. The large amount of high quality data requires much more sophisticated models for analysis than are currently available.

The type of model developed is a many particle-trajectory Monte Carlo model. The facility and economy of using this type of model for treating the complex geometry and dependencies mentioned above has been discussed and demonstrated in the published literature (Combi and Delsemme 1980a and 1980b, Combi 1980). The traditional approach initiated by Eddington's (1910) fountain model and continued in such later works by Haser (1957, 1966), Wallace and Miller (1958), Keller and Meier (1976) and Festou (1981) becomes computationally unmanageable for multi-dimensional time-dependent models. This is also true for the one-dimensional fluid models which have begun to model the physics correctly (Marconi and Mendis 1982, Huebner and Keady 1982).

During the first year of the project all of the new processes have been incorporated into the Monte Carlo particle-trajectory model (MCPTM). Preliminary analyses as to their effects on the spatial distributions of observed cometary radicals have been begun. These first exploratory model runs will be discussed in detail in the following sections of this report.

Also, in the interest of obtaining new data regarding the spatial distributions of neutral cometary species, a collaborative effort with Dr. Uwe Fink of the University of Arizona has been established.

II. Observations of the Spatial Distributions of Cometary Radicals

An important part of this project is to assess the observed spatial distributions of cometary radicals in order to constrain the parameters of the MCPTM. Most observations of this type have been analyzed in terms of Haser's (1957) model. Although Haser model scale lengths cannot be used to give direct physical quantities (lifetimes), they can be useful tools to characterize the apparent size of the source and decay regions of cometary radicals.

Newburn and Spinrad (1984) have presented Haser scale lengths for the parents of C_2, C_3 and CN in several periodic comets. These were obtained by two-point filter photometry: one point centered on the photometric nucleus and another displaced some known distance from the nucleus (typically 1 to 4×10^4 km). Since Haser's model is basically a three parameter model (the production rate and two scale lengths), Newburn and Spinrad had to assume the values of A'Hearn (1982) for the radical decay length. From two points they could then calculate both a parent scale length and the production rate. Although errors could arise from both this assumption and that of spherical symmetry (i.e., no radiation pressure distortion), a large number of observations may average out some of the random discrepancies.

Figure 1 shows a plot of the CN parent scale length versus heliocentric distance for the combined data sets of Newburn and Spinrad (1984), Combi and Delsemme (1980) and Delsemme and Combi (1983) as well as a newer value determined by Johnson, Fink and Larson (1984) from their CCD long-slit spectra of Comet P/Tuttle. There is no gross systematic difference between the two data sets. The scale lengths of Newburn and Spinrad were determined from the two-point photometry of smaller short period comets at medium to large heliocentric distances, whereas our data and that of Johnson, Fink and Larson were determined from the average of the sunward and antisunward brightness profiles of larger new or very long period comets at small to medium heliocentric distances. There are large uncertainties involved in determining one scale length from only two points. Newburn and Spinrad admit a factor of 2 change in the parent scale length results from a 25% change in one of the two measured fluxes. On top of this is their need to assume A'Hearn's adopted daughter scale length law for CN, where we (Combi and Delsemme 1980b) had found in fact no heliocentric distance-dependent law for CN but a distribution of values varying rather randomly over an order of magnitude. Therefore, the

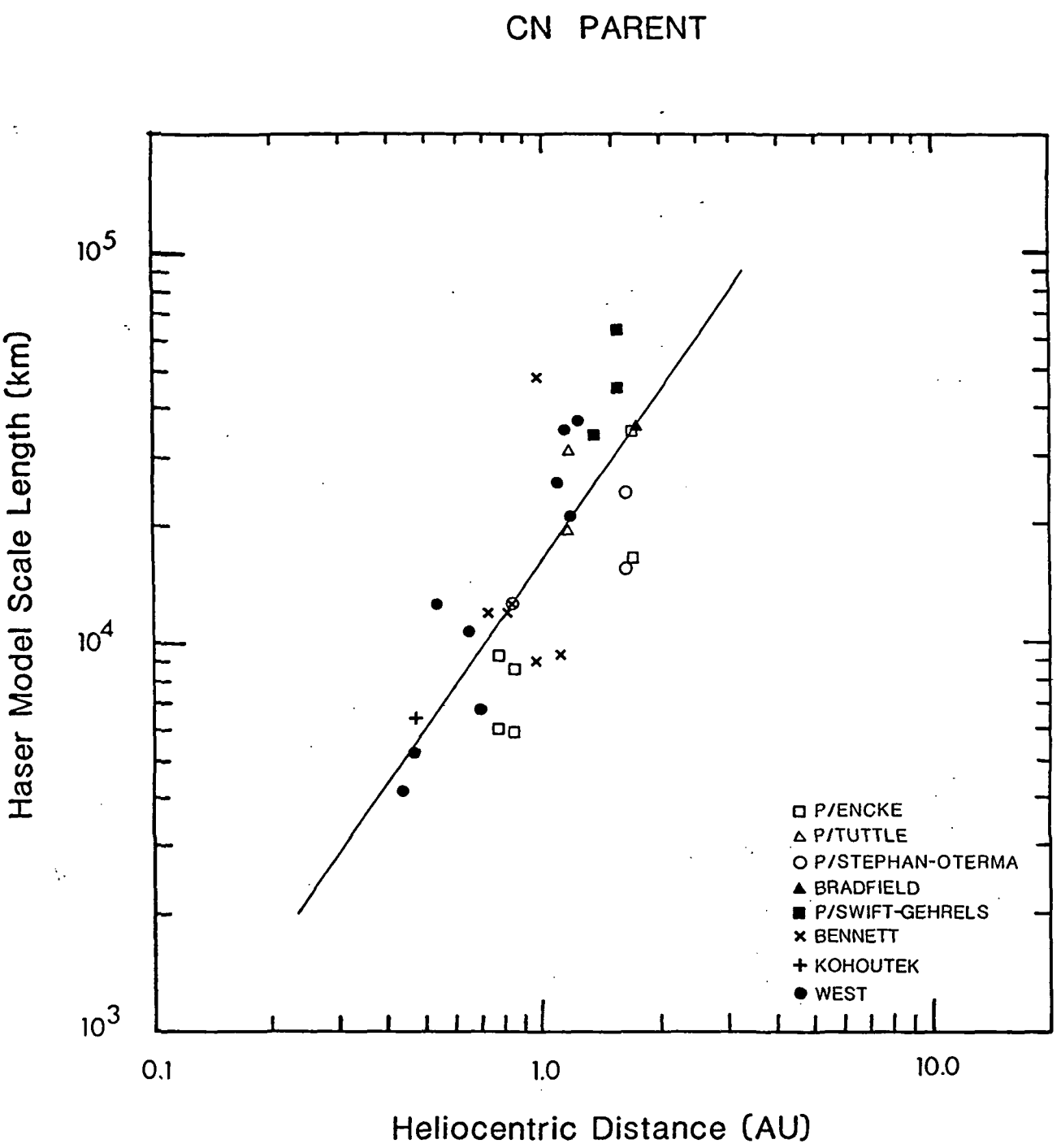

Figure 1. CN Parent Scale Length vs. Heliocentric Distance. The points plotted for Comets P/Encke, P/Tuttle, P/Stephan-Oterma and Bradfield were computed from two-point filter photometry by Newburn and Spinrad (1984). Those for Comets Bennett, Kohoutek and West were computed from entire brightness profiles (Combi and Delsemme 1980b, Delsemme and Combi 1983). The solid line is the best fit power law to the combined data sets.

facts that both sets of data indicate a similar r_H dependence and the mean values agree to within a factor of 2, are quite encouraging though possibly just fortuitous.

Taking all the data together, a power law can be fit which yields the straight line in Figure 1 and which has the form $\lambda_p = 1.6 \times 10^4 \, r_H^{1.44}$ for λ_p in km and r_H in AU. The slope for this fit has an uncertainty of about ±0.3 generally excluding both the typically adopted r_H^1 or r_H^2 laws. An $r_H^{1.5}$ law, on the other hand, would be expected for a photodissociation lifetime ($\tau \propto r_H^2$) and a variable parent velocity ($v \propto r_H^{-0.5}$).

Figure 2 shows the variation of the C_2 parent scale length with heliocentric distance for the combined data sets. Unlike the case for CN, though, there does seem to be a systematic difference. The scale lengths of Newburn and Spinrad tend to be both larger and exhibit a flatter slope than do those compiled by Combi and Delsemme (1985). Taken together, a power law in r_H can be fitted to all the data which have the form $\lambda_p = 2.2 \times 10^4 \, r_H^{1.9}$. The full profile data taken alone has the form $\lambda_p = 1.6 \times 10^4 \, r_H^{2.0}$, whereas the data of Newburn and Spinrad yield $\lambda_p = 3.8 \times 10^4 \, r_H^{0.7}$.

At this point, there could be two reasons for such a difference. First, the C_2 spatial distribution in the smaller short period comets may be substantially different from that in the more active new and very long period comets. If C_2 were produced primarily by gas phase chemical reactions or an icy grain source as suggested by A'Hearn and Cowan (1980), there could certainly be differences between the two populations of comets. Second, there could be differences between the two model fitting procedures. The C_2 radical experiences nearly twice the acceleration and is likely moving at a lower speed than is CN (Combi and Delsemme 1985). Since the two-point photometry method does not average out the asymmetry, systematic differences could result. In addition, the general problem discussed above where a modest uncertainty in one of the measured fluxes causes a large uncertainty in the determined scale length still applies. In any event, the C_2 results for complete brightness profiles seem to present a reasonable case for an r_H^2 law for the C_2 parent scale length.

Finally, for C_3 the only complete data are those by Newburn and Spinrad, which also seem to be consistent with something like and r_H^2 law for the parent Haser scale length given by $2.5 \times 10^3 \, r_H^2$ km.

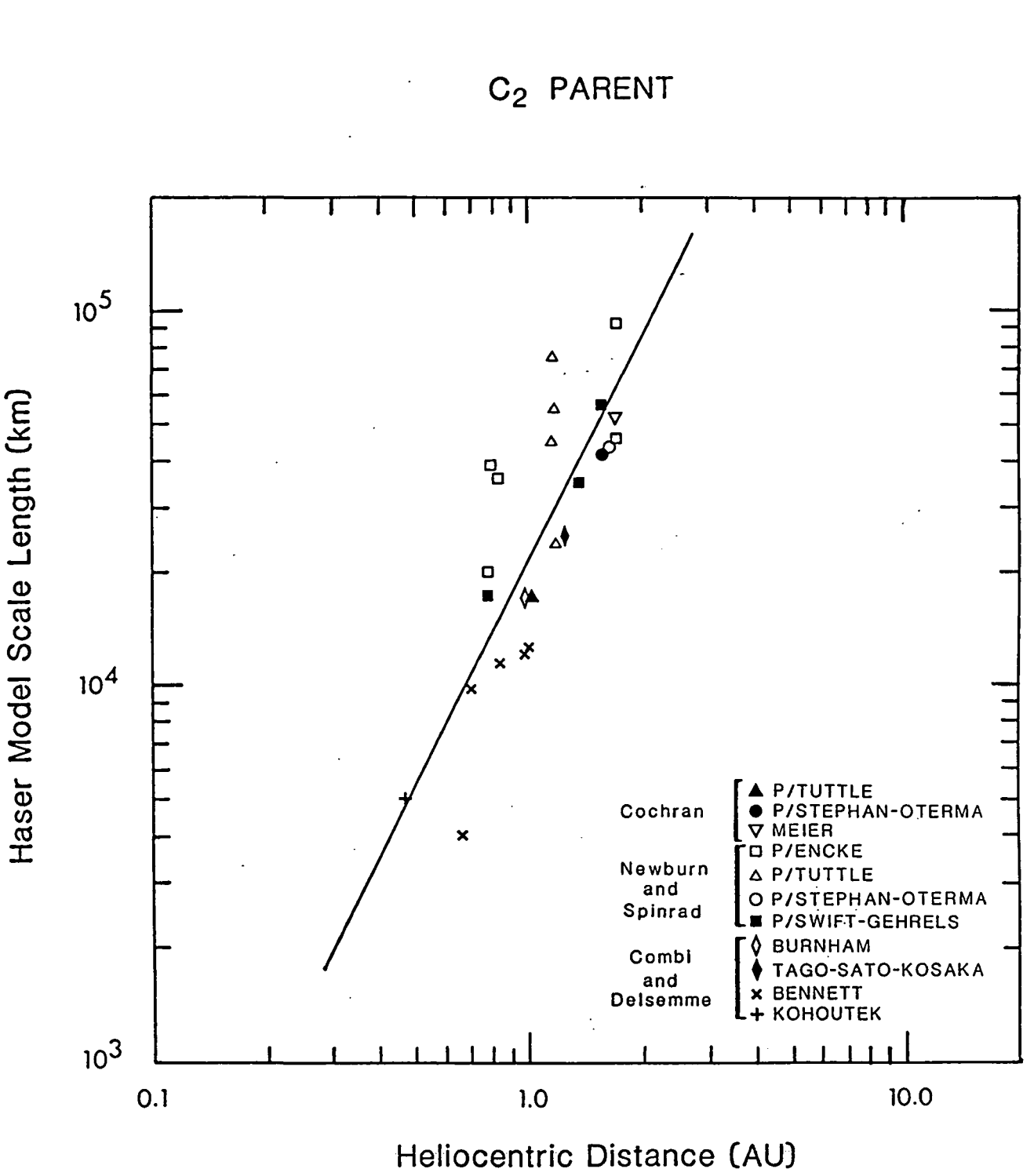

Figure 2. C_2 Parent Scale Length vs. Heliocentric Distance. The points plotted for Comets P/Encke, P/Tuttle, P/Stephan-Oterma and P/Swift-Gehrels were computed from two-point filter photometry by Newburn and Spinrad (1984). Those for Comets Burnham, Tago-Sato-Kosaka, Bennett and Kohoutek were computed from entire brightness profiles (Combi and Delsemme 1985). The solid line is the best fit power law to the combined data sets.

III. Photochemical Data

Another important aspect of modelling the spatial distributions of cometary radicals is the photochemical data relevant to the photodestruction (dissociation and/or ionization) of radicals and their prospective parents, as well as the fluorescence emission rate per indicent solar radiation flux (or g-factor).

CN.

Because of the existence of many solar absorption lines in the region of ~ 3900A°, the g-factor for the CN(0-0) is not only a function of heliocentric distance (~ $1/r_H^2$) but is also a rather strong function of heliocentric velocity (the Swings effect). This calculation has been performed by Tatum and Gillespie (1977) and Mumma et al. (1978). Both calculations demostrate the same relative heliocentric velocity dependence but differ by an overall factor of ~ 20% due to the respective use of disk center and disk average solar spectra (see A'Hearn 1982 for a plot of the two calculations). Figure 3 shows a plot of the calculation of Tatum and Gillespie adopted here as the only formally published data. The g-factor is not only important for calculating absolute column densities but also because it directly contributes to the radiation pressure acceleration which visibly distorts the CN coma (Combi 1980).

Our initial suggestion for HCN as the parent of CN (Combi and Delsemme 1980b, Combi 1980) has remained a quite viable explanation of the observed brightness distribution. Cochran (1982) has reached a similar conclusion from observed brightness profiles of CN in Comet P/Stefan-Oterma. Huebner (1985) has recently revised the photochemical lifetime of HCN downward only slightly from 8.3 x 10^4s (Huebner and Carpenter 1979) to 7.7 x 10^4s, with the major contribution still from solar Lyman α. As before, an excess energy of 4.3eV divided among the fragments yields a random velocity for CN radicals of 1.1 km/s with respect to the radially outflowing HCN molecules.

C_2.

The g-factors for the various bands of the Swan system of C_2 are relatively well known and there seems to be no significant heliocentric velocity dependence (A'Hearn 1975, A'Hearn 1982, Danks and Lambert 1983). The case for identification of the production mechanism for C_2 (i.e., possible parent

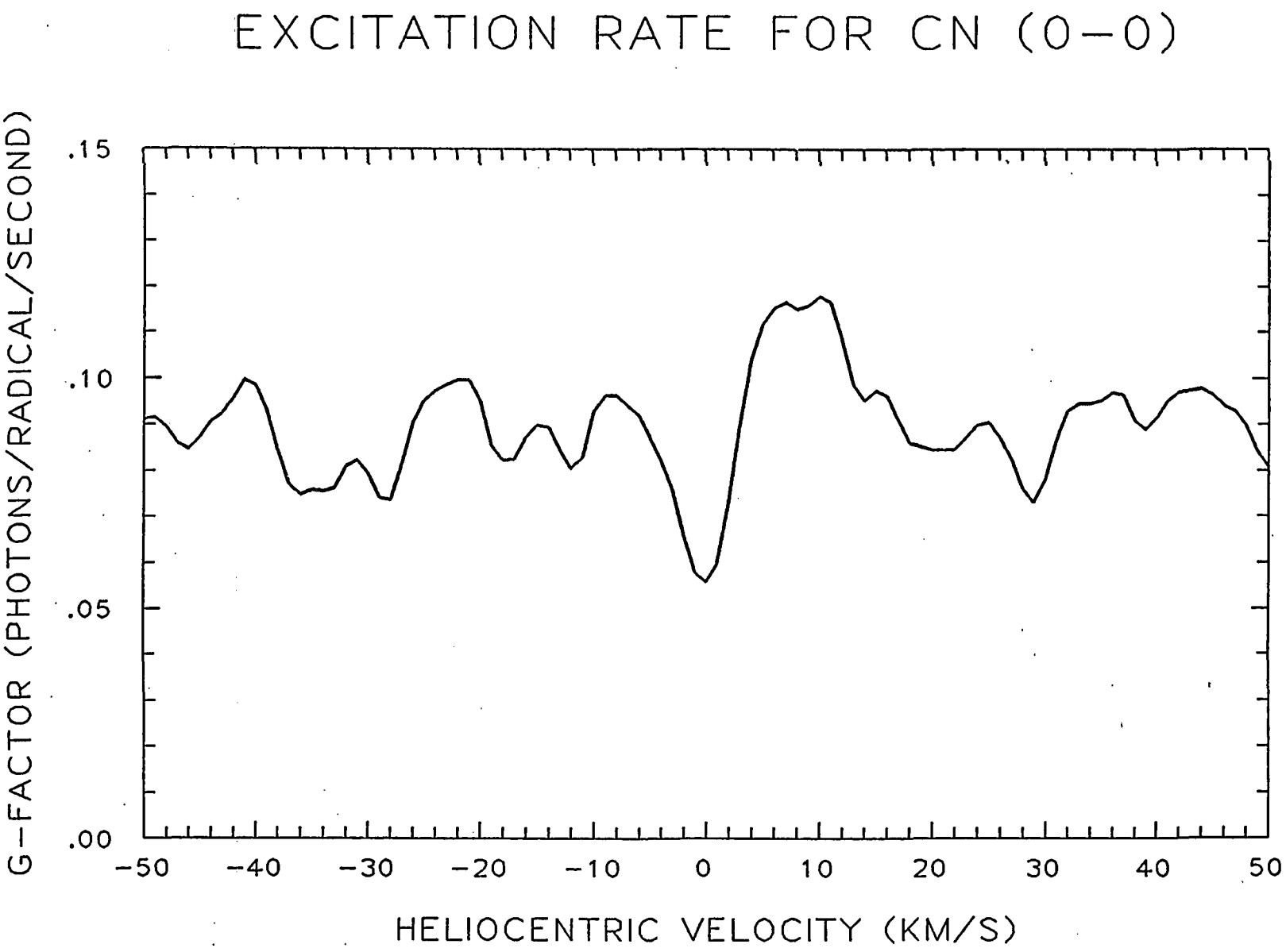

Figure 3. Fluorescence Excitation Rate for CN(0-0) at 3883 Å. Plotted is the excitation rate (g-factor for the (0-0) band of CN at 3883 Å as a function of heliocentric velocity as computed by Tatum and Gillespie (1977).

molecules) is, however, not so advanced. A recent paper by Cochran (1985) has advanced the theory that the shape of three C_2 brightness profiles in three different comets can be explained by the photodissociation chain $C_2H_2 \rightarrow C_2H \rightarrow C_2$ provided that the unknown lifetime of C_2H is about 2000 seconds. This conclusion was based on a one-dimensional single-fluid chemical model (Cochran 1982) which included the estimation of the C_2H_2 photodissociation lifetime of 3.2×10^4 seconds originally calculated by Huebner and Carpenter (1979). The conclusion then really implies that effective parent lifetime for production of the C_2 radical is of order 3.4×10^4s and that the lifetime of C_2H must be negligible (2000s) as compared with that for C_2H_2 itself ($\sim 3.2 \times 10^4$s). Very recently, however, Huebner (1985) has revised the early study of acetylene photochemistry and finds the following branches and rates are dominant:

$$C_2H_2 + h\nu \rightarrow C_2H + H \qquad \tau^{-1} = 1 \times 10^{-5}\,s^{-1}$$
$$\rightarrow C_2 + H_2 \qquad \tau^{-1} = 2.7 \times 10^{-6}\,s^{-1}.$$

Therefore, the new lifetime for acetylene is 7.9×10^4s, which is more than a factor of two larger than that implied by the observed profile. This would seem to <u>eliminate</u> C_2H_2 as the only or even primary parent for C_2.

C_3.

Very little is known photochemically about C_3 or prospective parents. The g-factor for the $A^1\Pi_u \rightarrow X^1\Sigma_g^+$ band at 4040A° has recently been revised upward by a factor of 40 (A'Hearn 1982). Thus, instead of being as nearly abundant as C_2 and CN as was believed, production rates are now reduced to over an order of magnitude less. One implication of this is that C_3 can no longer contribute significantly as a source of C_2 by photodissociation. Another is that the radiation pressure acceleration of C_3 radicals by solar light can now be calculated to be .56 cm s^{-2}, which is larger than both C_2 and CN, .42 and .34 cm s^{-2} respectively.

The simplest prospective parent for C_3 for whose photochemical lifetime has been calculated is CH_3C_2H (propyne). Stief (1972) has suggested the following reaction chain in which propyne is photodissociated leaving C_3H_2 in an excited state that spontaneously decays to form C_3:

$$CH_3C_2H + h\nu \rightarrow C_3H_2^* + H_2$$
$$C_3H_2^* \rightarrow C_3 + H_2$$

Stief found a rough lifetime for this reaction of 5000s, which is actually reasonably consistent with the Haser scale length of 2.5×10^3 km found by Newburn and Spinrad (1984, see Section II) for an expected parent velocity of $\sim.58$ km s^{-1}.

OH.

Schleicher and A'Hearn (1982, 1984) have calculated the dependencies of both the OH photodissociation lifetime and the OH solar fluorescence rate on heliocentric velocity. At a distance of 1 AU from the sun, the OH lifetime can vary from $\lesssim 2 \times 10^5$ s to $\sim 4 \times 10^5$ s depending on the heliocentric velocity. The (0-0) band fluorescence rate varies by more than a factor of 6 for different heliocentric velocities. Figures 4 and 5 show these dependencies which have been incorporated in to the cometary radical particle-trajectory model. It is important to note that these calculations are made only for transitions between the ground $X^2\Pi$ and the $A^2\Sigma^+$ electronic states. Fluorescence occurs for transitions up to the $v' = 0$ and 1 vibrational levels, and predissociation occures for $v' \geq 2$. Furthermore, Singh, van Dishoeck and Dalgarno (1983) point out possible transitions to other electronic states with an important role for Lyman α absorption. Van Dishoeck and Dalgarno (1983) suggest a combined rate of $3.8 \times 10^{-6} s^{-1}$ for these other states. Simply adding the rates from the two calculations together would yield a total photodissociation lifetime in the range of only 1 to 1.6×10^5s, also decreasing the magnitude of the heliocentric velocity dependence. However, Schleicher (1983) points out that Festou (1981b) using the vectorial model and the correct kinematics for H_2O photodissociation finds lifetimes for OH in the range of $2\text{-}3 \times 10^5$s, apparently just in the range predicted by the Schleicher and A'Hearn calculation alone.

IV. The New Monte Carlo Particle-Trajectory Model

The original Monte Carlo particle-trajectory model (MCPTM) as developed by Combi and Delsemme (1980a) has been generalized during the first year of this project and now includes:

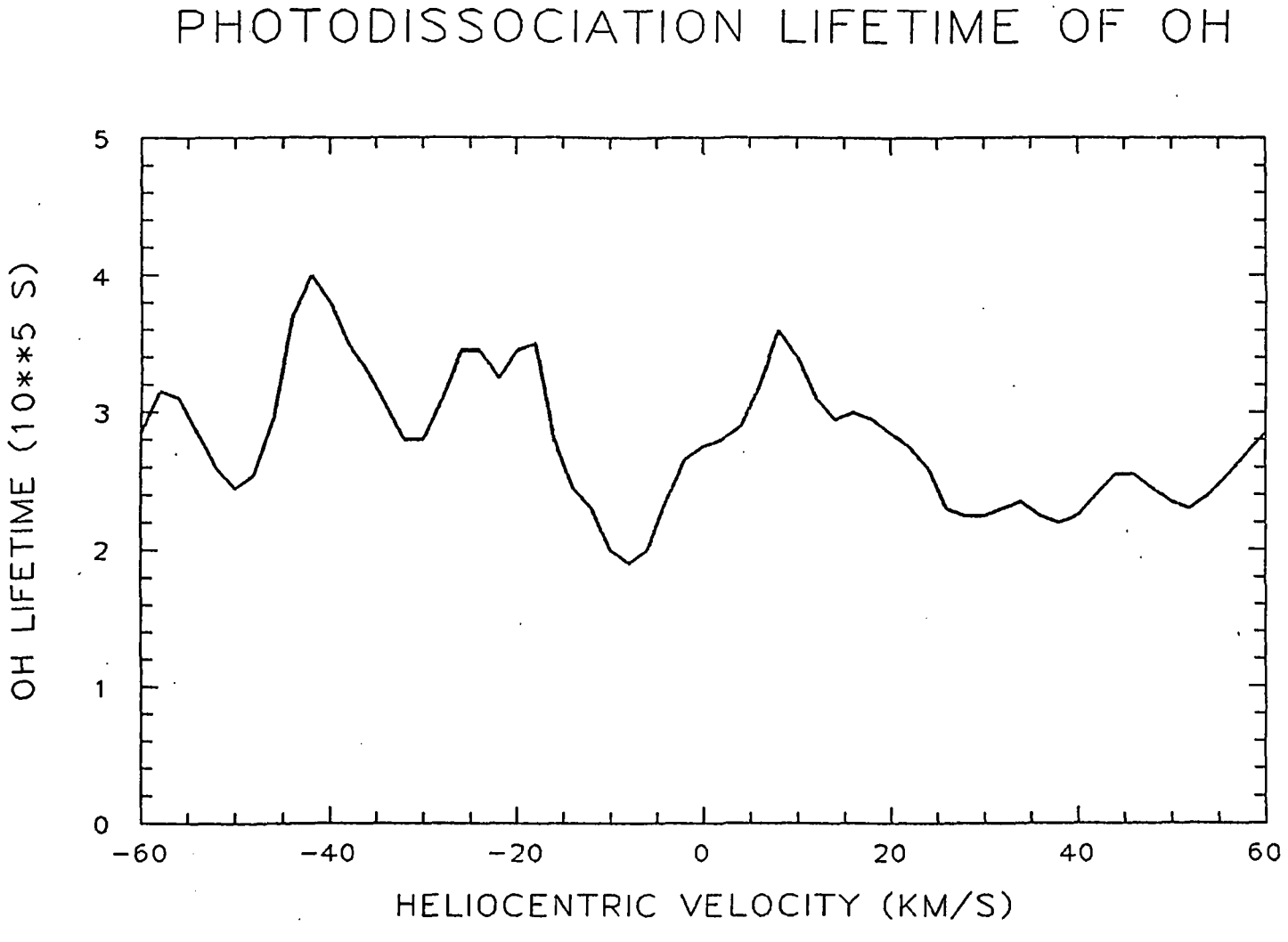

Figure 4. Photodissociation Lifetime of OH as a function of Heliocentric Velocity (Schleicher and A'Hearn 1982).

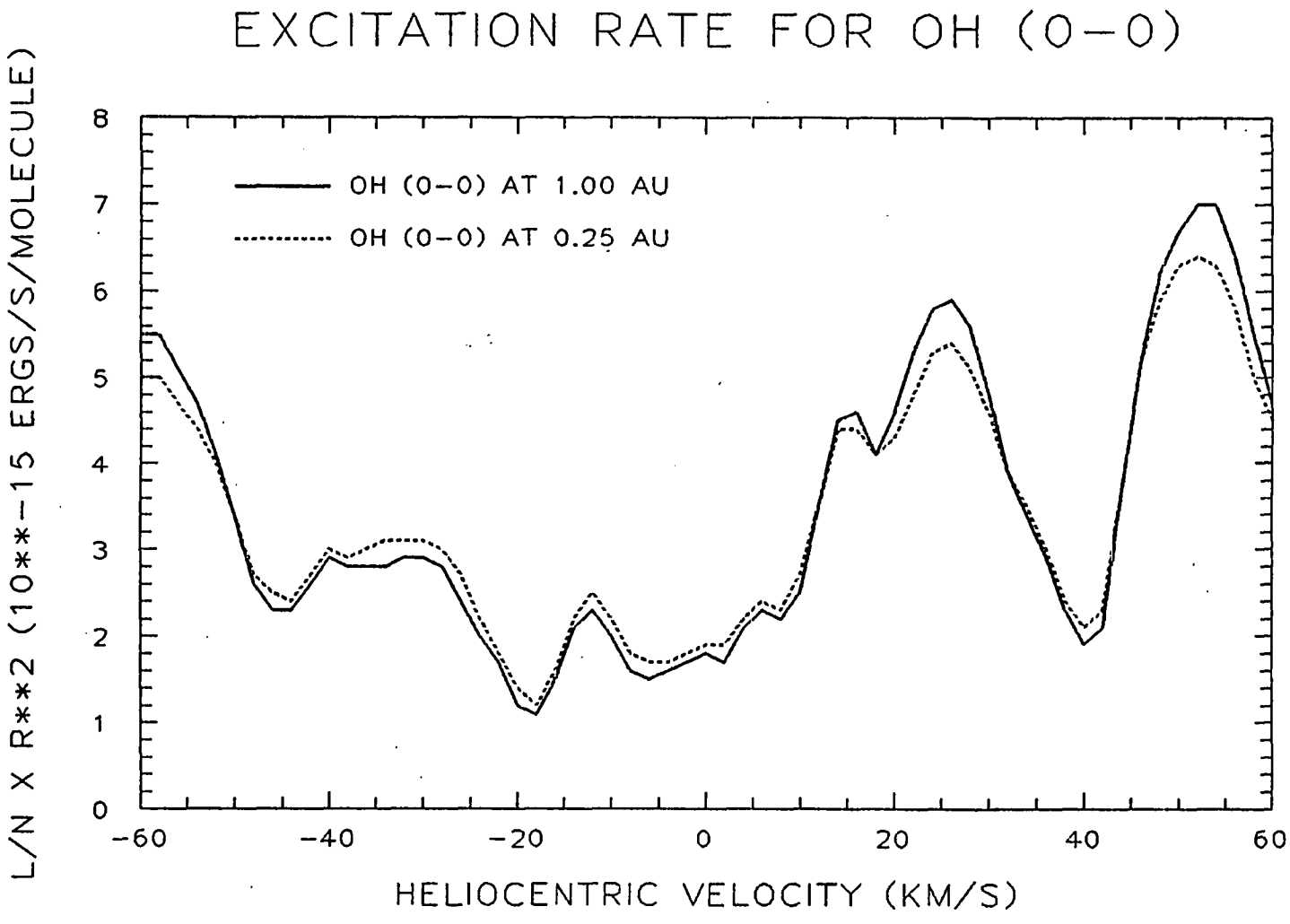

Figure 5. Excitation Rate for the OH(0-0) Band. The heliocentric velocity dependence is shown for heliocentric distances of 0.25 AU and 1.00 AU (Schleicher and A'Hearn 1984).

(1) solar radiation pressure

(2) isotropic ejection of daughter radicals owing to excess photolysis energy,

(3) the heliocentric distance dependent parent velocity (Delsemme 1982),

(4) time (heliocentric distance) dependent source rate and lifetimes,

(5) heliocentric velocity dependent lifetimes and excitation rates, and,

(6) multiple elastic scattering of cometary radicals by the outflowing gas.

As each new process was incorporated into the MCPTM, exploratory model runs were made in order to test the effect of the process on the observed spatial distribution. I will now present separate discussions for each new physical process giving a brief description of the modeling procedure and some preliminary model results.

A. Radiation Pressure and Variable Parent Outflow Velocity

Although the original model included radiation pressure (also see Combi 1980), a constant velocity for the outflowing parent molecules had been assumed. Furthermore, no calculations had ever been carried out to invert nucleus-centered filtered photometric observations with a model which included both the isotropic ejection of daughter radicals (also as in the vectorial model) and radiation pressure. As mentioned in Section II of this report, Haser parent scale lengths determined from observed CN profiles indicate something like an $r_H^{1.5}$ law. This would be expected for the photodissociation of parent molecules combined with the outflow velocity law determined semi-empirically by Delsemme (1982) to be $v = .58\ r_H^{-1/2}$ km s^{-1}. The production rates for CN as determined from the photometry of Comet West (1976VI) (A'Hearn et al. 1977, A'Hearn and Cowan 1980) have been recalculated for various model process combinations in order to test their effects.

A'Hearn et al. (1977) had originally used an r_H^{+1} law for a Haser model parent scale length for CN and found that the production rate for CN varied with heliocentric distance as $r_H^{-2.8}$. Combi and Delsemme (1980b) then measured CN parent scale lengths in Comets Bennett and West and found a dependence of $r_H^{1.8\pm.1}$ which they concluded was reasonably consistent with an r_H^2 law. Both they and A'Hearn and Cowan (1980) then adopted the r_H^2 law and found a CN production rate varying approcimately as r_H^{-n} where $n \approx 1.6\pm0.3$.

For this study, the CN production rates have been calculated using three different model descriptions and compared with the Haser model parameters

A'Hearn and Cowan have adopted. The results of these four cases are shown in Table 1. The first case is a Haser model, using the Average Random Walk Model (Combi and Delsemme 1980a) corrections to the scale lengths. Here the r_H variation in parent velocity and the isotropic ejection of the daughter radicals is taken into account in an approximate way. The second case is a Monte Carlo Particle Trajectory Model (MCPTM) which explicitly calculates the effects included in the first case. And the third case is a MCPTM which also includes radiation pressure (Combi 1980). In all cases the heliocentric velocity dependence of the CN(0-0) band excitation (Tatum and Gillespie 1977) is included.

The largest effect is that of the variation of the parent velocity which steepens the slope of the resulting production law and is present in all three cases. The explicit inclusion of isotropic ejection (case 2) and radiation pressure (case 3) each flatten the slope somewhat but are nonetheless important. A comparison of the original Haser model calculations and the full MCPTM (Case 3) for the CN production in Comet West is shown in Figure 6.

B. Multiple Elastic Scattering of Cometary Radicals

Models of neutral cometary comae have generally dealt with the two extreme cases: one where the densities are high enough so that all neutral species are thermalized and are characterized by a bulk radial flow away from the nucleus (e.g., one-dimensional fluid models by Giguere and Huebner 1978, Marconi and Mendis 1982, Cochran 1982), and the other where the densities are so low that essentially no collisions occur (e.g., the vectorial model by Feston 1981a).

A characteristic distance from the nucleus separating these two regions has been defined where the mean free path for a collision is equal to the distance from the nucleus. Whipple and Huebner (1976), for example, express this collision radius as

$$r_c = \frac{Q\sigma}{4\pi v}$$

where Q = molecular production rate

σ = cross-section for elastic scattering $\sim 10^{-15}$ cm^2

v = molecular outflow velocity.

Table 1

CN Production in Comet West

	Model	Q_1 $(s^{-1})^{(a)}$	n (b)
	A'Hearn and Cowan Haser Model	1.1×10^{27}	-1.61
1)	Average Random Walk Model	1.4×10^{27}	-2.00
2)	Monte Carlo Particle Trajectory Model (no radiation pressure)	1.2×10^{27}	-1.92
3)	Monte Carlo Particle Trajectory Model (with radiation pressure)	1.3×10^{27}	-1.87

(a) Production Rate at 1 AU

(b) Exponent in power law $Q = Q_1 \, r_H^{\,n}$

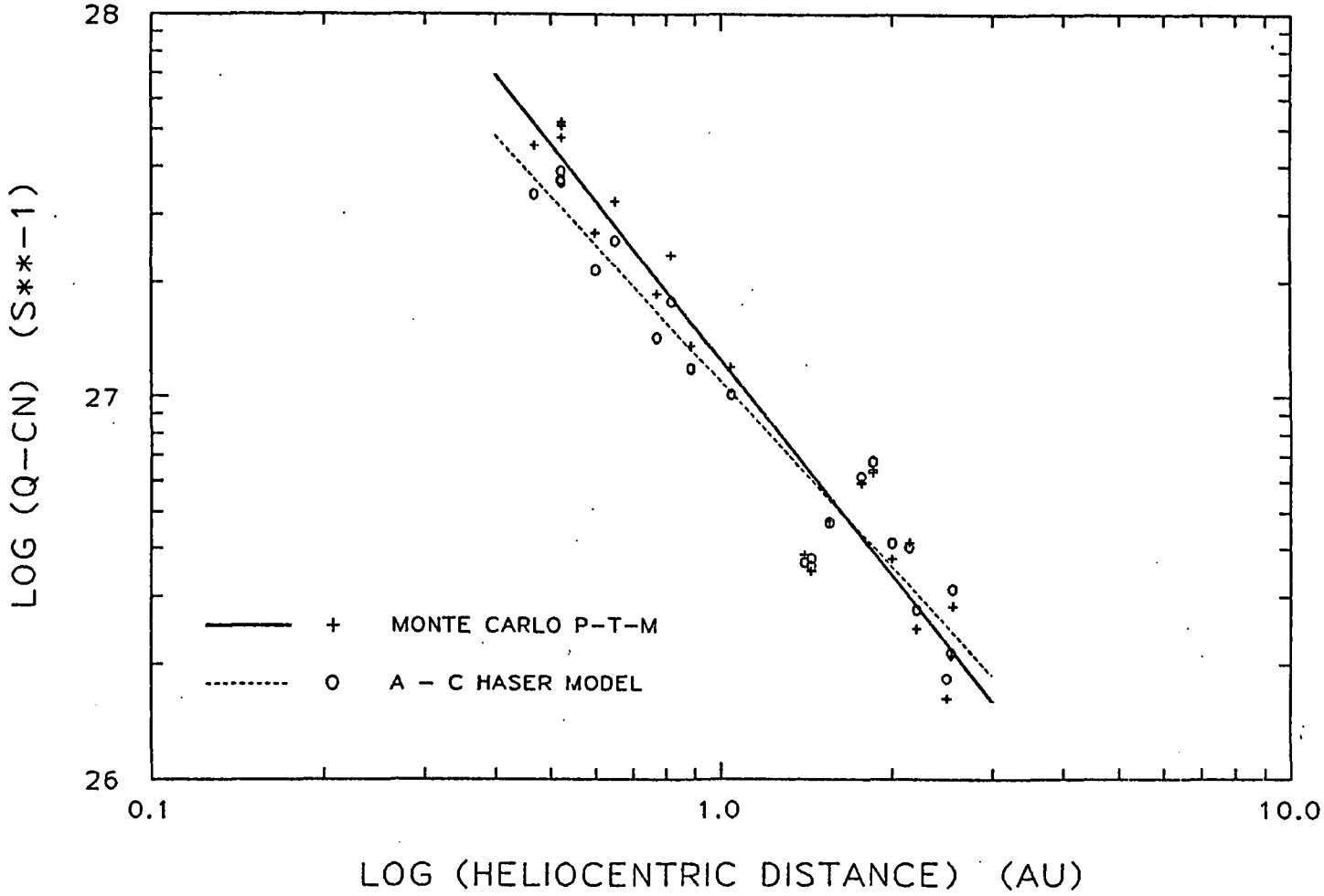

Figure 6. CN Production Rate vs. Heliocentric Distance. The CN Production rates for Comet West are shown as computed both with the Haser model scale lengths of A'Hearn and Cowan (1980) [O] and with the Monte Carlo particle trajectory model which includes radiation pressure and a variable parent velocity [+]. Intermediate cases are discussed in the text.

The value of r_c varies from $\sim 10^4$ km for a bright comet like Kohoutek near perihelion, down to $\sim 10^2$ km for a small short period comet like P/Encke at 1 AU.

In reality, though, there is no clear separation between the two zones. In order for a typical radical (CN, C_2, OH) which has been emitted from its parent with some exothermic velocity to be truly thermalized, it needs on the order of 10 collisions with outflowing water molecules. On the other hand, many radicals produced outside of r_c will be subjected to at least 1 to 5 collisions, thus questioning the true applicability of a free flow model. What we truly have, then, is a large regime on the order of 0.2 r_c to 5 r_c where partial thermalization will occur.

The true random walk nature of the elastic scattering problem is modeled in a straightforward manner in the Monte Carlo particle-trajectory model (MCPTM). Kitamura et al. (1983) have included collisions in a Monte Carlo model essentially based on our original model (Combi and Delsemme 1980a). Since they basically followed the correct procedure, we have adopted a similar algorithm. There is one problem with their procedure which involves the expression they assume for the density of outflowing molecules with which the modeled neutral radicals are colliding. They assume a Haser-like description for the density which is

$$n_{H_2O}(r) = \frac{Q}{4\pi v} \frac{1}{r^2} \exp(-r/v\tau_{H_2O})$$

where Q, v are as above

r = distance from the nucleus

τ_{H_2O} = photochemical lifetime for H_2O.

Strictly speaking, this is the correct density distribution for H_2O molecules, but as the H_2O molecules dissociate, they produce OH and H, which still provide targets with which radicals collide. Since the effective cross-sectional area for the fragments is larger than the parent H_2O but their outflow velocity is, on the average, also larger, a better approximation would be to simply drop the exponential term in the density expression. This yields

$$n_{H_2O}(r) = \frac{Q}{4\pi v r^2} .$$

For the simple case of no radiation pressure, this yields a closed form algebraic expression for the collision length of an arbitrarily moving neutral species, in place of the integral found by Kitamura et al. For the radiation pressure case the parabolic trajectory is divided into finite elements each of which is treated as a straight-line case.

The random walk algorithm begins with the production of a neutral radical by its parent with a given velocity vector. From this location and velocity vector, a collision length is given by assumed values for the collision cross section, the molecular (H_2O) production rate, and a random number. The neutral is then displaced this distance, scattered elastically off a moving water molecule and continued on for another collision. The trajectory proceeds this way until the observation time snap-shot.

Preliminary model runs have been performed for the case of CN produced by the photodissociation of HCN (Combi and Delsemme 1980b). We have chosen parameters appropriate for the photochemical lifetimes at 1 AU and have neglected radiation pressure, which is of less importance at 1 AU, for the purpose of simplifying the preliminary analysis. The physical parameters of the coma models are:

$$r_H = 1 \text{ AU}$$
$$\tau(\text{HCN}) = 9 \times 10^4 \text{ s}$$
$$\tau(\text{CN}) = 2.75 \times 10^5 \text{ s}$$
$$v(\text{parent}) = 0.58 \text{ km/s}$$
$$v_e(\text{CN}) = 1.02 \text{ km/s}$$
$$\sigma_{\text{scattering}} = 1 \times 10^{-15} \text{ cm}^{-2}$$

Models were run for cases of general molecular production rates from 1×10^{28} s^{-1} to 1×10^{30} s^{-1}. The collision statistics from these model runs summarized in Table 2. As can be seen, for larger gas production rates, only half of the CN radicals produced are in a true free-flow regime. Furthermore, the effect collisions have on the determination of radical production rates is also evident in these model runs. For the case of the largest gas production rate, if one neglects collisions in the model, an underestimate of 11% to 15% in the determination of radical production rate would be made, depending upon the size of the photometer aperture used. The systematic errors, when reducing data for even smaller heliocentric distances ($r_H \sim 0.5$ AU), should be

Table 2

Collision Statistics for the CN Model at 1 AU

	Fraction of Radicals Undergoing n Collisions				
Q_{H_2O} \ n	0	1-2	3-5	6-10	>10
1×10^{28}	.723	.272	.0042	.0005	.0003
5×10^{28}	.705	.283	.0094	.0023	.0005
1×10^{29}	.681	.296	.0160	.0055	.0009
2×10^{29}	.653	.311	.0247	.0101	.0016
5×10^{29}	.576	.343	.0503	.0252	.0055
1×10^{30}	.503	.355	.0852	.0459	.0147

quite important in bright comets such as P/Halley, since at these distances the collisional effects are compounded by larger gas production rates and smaller radical parent scale lengths.

C. Time Dependence

Time dependence in comet model parameters such as production rate, photochemical lifetimes and velocities enters naturally through the changing of the comet's heliocentric distance and velocity along its orbit with time. Models by Keller and Meier (1976) and Cucchiaro and Malaise (1982), for example, have treated time-dependent production rates, with the former also treating the time-dependent hydrogen lifetime and radiation pressure acceleration. As part of this project, however, time dependence has been included in all aspects of the extended source, kinematics, and decay of observed cometary radicals. The ability to handle such a general calculation illustrates the power of particle-trajectory models using Monte Carlo techniques.

The original calculation, described in detail by Combi and Delsemme (1980a), and since then adopted by others (see Bockelee-Moran and Gerard 1984, Kitamura, Ashihara and Yamamoto 1985, and Schloerb and Gerard 1985), correspond to steady-state production rates and constant photochemical lifetimes for parent (and grandparent) and daughter species. Typically, N ($\sim 10^5$) parent molecules are emitted at random times between the current or observation time and some back-up time t_B which is long enough to build up the whole observed cloud. In this case, the model production rate is given simply by N/t_B, which may be simply scaled to the desired production rate or fitted to an observation to yield the production rate. Given typical random numbers (R_i) on the interval [0,1) the back-up time for emission of a parent is given by $t_I = R_i t_B$.

In the steady-state MCPTM the manner in which the constant lifetimes for both parent and daughter decay has been modified from the original model in the interest of improving the statistical coverage. In the old procedure a decay time was computed using the principal of Monte Carlo, which yields the relation $t_D = -\tau \ln (1-R_i)$ where τ is the exponential decay lifetime. This was computed twice, once for the parent and once for the daughter; a daughter trajectory was only computed only if the parent decay occurred within a time t_I and the daughter decay did not. A better method is to use the concept of a forced dissociation for the parent and a simple weighting function for the

daughter decay (see forced first scattering discussion by Cashwell and Everett 1959). A parent dissociation within the time t_I is given by

$$t_D = -\tau_p \ln \cdot \left(1 - R_i \left[1 - e^{-t_I/\tau_p}\right]\right)$$

and the daughter is assigned a weight ($\neq 1$) given by

$$w = \left(1 - e^{-t_I/\tau_p}\right) e^{-(t_I - t_D)/\tau_d}$$

where τ_p and τ_d are the parent and daughter decay lifetimes. The first term (in parentheses) results simply from the forced parent dissociation. In the steady-state MCPTM the trajectories are calculated and collected in space and column density bins as before.

In the time-dependent model, the variable production rate is treated quite simply by weighting a parent molecule according to the production rate at the emission time ($t_{observation} - t_I$) relative to the production rate at the observation time. Thus a water vaporization curve or a simple power law in heliocentric distance can be assumed; for that matter, transient activity or outbursts can also be accounted for by simple weighting.

The variable lifetime for the parent and daughter decay are somewhat more involved. The generally time-dependent lifetimes $\tau = \tau(t)$ can be approximated as a set of finite element steps

$$\tau = [\tau_1(T_1),\ \tau_2(T_2),\ \tau_3(T_3),\ \ldots,\ \tau_n(T_n)]$$

where $(T_1,\ T_2,\ T_3, \ldots T_n)$ are sub-intervals in time such that

$$T_1 + T_2 + T_3 + \ldots + T_n = t_I .$$

The partial weight associated with the forced dissociation is then given by

$$W_D = 1 - \exp[-(T_i/\tau_i + T_2/\tau_2 + T_3/\tau_3 + \ldots + T_n/\tau_n)] \ .$$

The probability for a dissociation somewhere on this interval $0 \leq t_D \leq t_I$ is

$$P(t_D) = 1 - e^{-\rho}$$

where $$\rho = \frac{T_1}{\tau_1} + \frac{T_2}{\tau_2} + \ldots \frac{T_{m-1}}{\tau_{m-1}} + t_D - \frac{(T_1 + T_2 + \ldots + T_m)}{\tau_m}$$

and $$T_1 + T_2 + \ldots + T_m \leq t_D \leq T_1 + T_2 + \ldots + T_m + \ldots + T_n .$$

The quantity, ρ, is just the number of mean free times (like mean free paths) contained in time t_D.

Just as in the steady-state case, the random number enters as the fraction of parents remaining after the time t_D; therefore,

$$R_i = (1 - e^{-\rho})/W_D$$

and solving for ρ we have

$$\rho = -\ln (1 - R_i W_D) .$$

Finally, t_D is determined from the inequality

$$\frac{T_1}{\tau_1} + \frac{T_2}{\tau_2} + \ldots + \frac{T_{m-1}}{\tau_{m-1}} < \rho \leq \frac{T_1}{\tau_1} + \frac{T_2}{\tau_2} + \ldots + \frac{T_m}{\tau_m}$$

and the equation .

$$t_D = T_1 + T_2 + \ldots + T_{m-1} + \tau_m \left[\rho - \left(\frac{T_1}{\tau_1} + \frac{T_2}{\tau_2} + \ldots + \frac{T_{m-1}}{\tau_{m-1}}\right)\right] .$$

Once t_D is determined, the daughter decay partial weight can be calculated in a more straightforward manner by simply summing up the partial exponential weights for the remaining intervals from T_m up to T_n.

$$W_d = \exp \left[\frac{-\tau_m\left(\frac{T_1}{\tau_1} + \frac{T_2}{\tau_2} + \ldots + \frac{T_m}{\tau_m} - \rho\right)}{\tau_m \text{ (daughter)}} + \right.$$

$$\left. \frac{T_{m+1}}{\tau_{m+1}\text{(daughter)}} + \ldots + \frac{T_n}{\tau_n\text{(daughter)}}\right] .$$

The trajectory calculation proceeds generally as before (Combi and Delsemme 1980a, Combi 1980) except that the radiation pressure acceleration is also time dependent (through the heliocentric distance and velocity) in general and

must also be calculated in finite time steps. This calculation proceeds as the daughter weight terms are summed.

A few preliminary model runs have been made with the new time dependent model. As one might expect, if one looks at densities or column densities reasonably close to the nucleus ($\lesssim 10^4$ km), there is little difference from a simple steady-state model. This first-order equivalence is due to the fact that as the comet changes heliocentric distance, photochemical lifetimes and parent molecule production rates change in opposite directions, tending to cancel each other. This cancellation also depends upon the production rate variation assumed in the model. If a simple inverse square law is assumed, as is true for small heliocentric distances ($r_H < 0.7$ AU) in the case of water vaporization or for the case of vaporization of something more volatile such as CO or CO_2, the cancellation in the absence of radiation pressure is very strong. However, for a true water vaporization curve, the time dependence in the model becomes much more important.

Figure 7 shows calculations for the CN coma as produced by HCN photodissociation with the new time dependent MCPTM at a heliocentric distance of 1 AU at times both pre- and post-perihelion. The orbit of Comet West was assumed as before; also, the vaporization curve for a dusty H_2O nucleus (Weissman and Kieffer 1984) was adopted. These model results at 1 AU imply an overall asymmetry of 10 percent in the range of 10^4 to 10^5 km usually covered by photometric apertures. The asymmetry increases to 20 percent for similar model runs at 2.5 AU.

Perhaps the importance of time dependence is more in the interpretation of the limited spatial distribution data which are used to characterize the Haser scale lengths photometric observers typically use to reduce their data. Daughter scale length determinations are usually quite sensitive to the outer portion of a brightness profile, and this is just the region where time dependence (or really its usual neglect) is important. Figure 8 shows the sunward and antisunward brightness profiles for the same two model runs as above. As in the case for collisions, radiation pressure seems to enhance also the effect of time dependence on the CN spatial distribution, especially for the sunward profile.

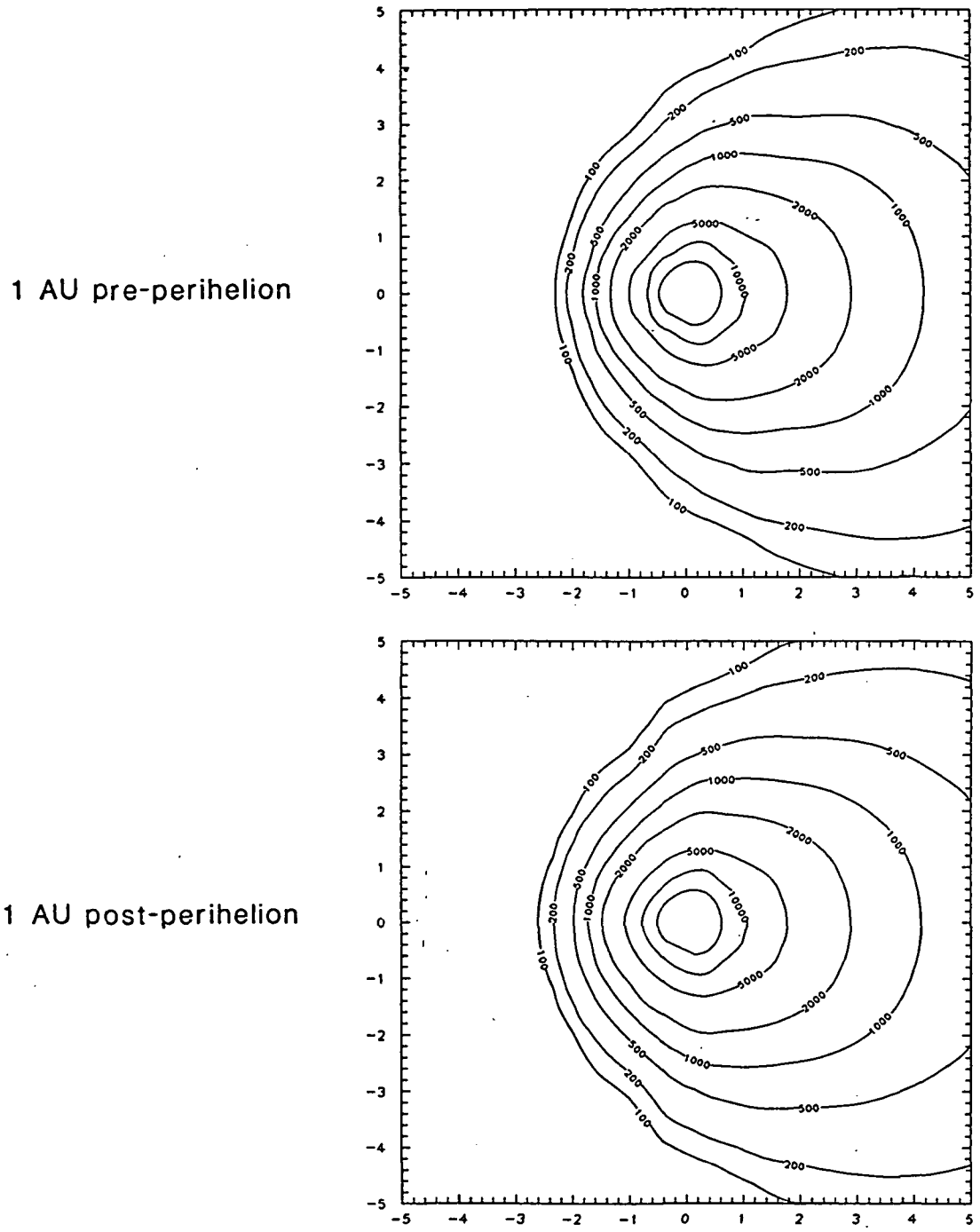

Figure 7. CN(0-0) Intensity Maps for Comet P/Halley at 1 AU Pre- and Post-Perihelion. These maps were computed with the new time dependent Monte Carlo particle-trajectory model for the orbit of Comet P/Halley assuming a water vaporization curve and the same production rate for CN of 1×10^{27} s^{-1}. The asymmetry introduced by the time dependence is most noticeable in the sunward direction and decreasing as one approaches the antisunward direction. The same g-factor was assumed for both maps in order to illustrate the actual abundance asymmetry.

Modeled CN(0-0) Brightness Profiles

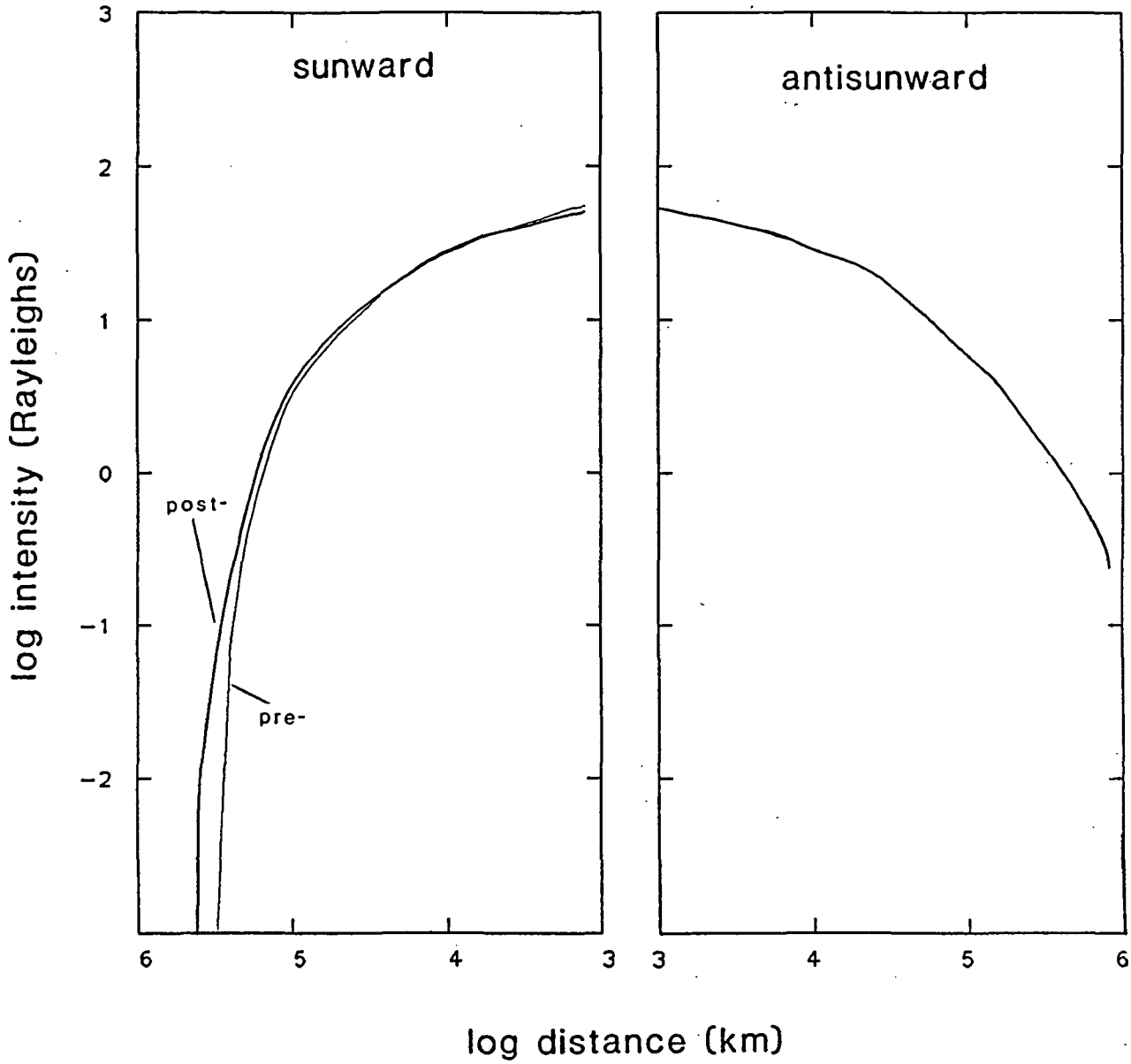

Figure 8. Sunward and Antisunward Brightness Profiles for CN(0-0) in Comet P/Halley at 1 AU Pre- and Post-Perihelion. As seen in Figure 7, the pre- to post-perihelion asymmetry is not present exactly antisunward but is quite noticeable in the sunward direction. See the caption for Figure 7 for modeling details.

References

A'Hearn, M.F (1975) A. J. 80, 861.

A'Hearn, M.F. (1982) in Comets (ed. L. Wilkening), The University of Arizona Press, Tucson AZ, pp. 433-460.

A'Hearn, M.F., and J.J. Cowan (1980) The Moon and Planets 23, 41.

A'Hearn, M.F., R. L. Millis and C.H. Thurber (1977) A. J. 82, 518.

Bockelee-Moran, D., and E. Gerard (1984) Astron. Astrophys. 131, 111.

Cashwell, E.D., and Everett, C.J. (1959) The Monte Carlo Method for Random Walk Problems. Pergamon Press, New York.

Cochran, A. (1982) Ph.D. thesis, University of Texas.

Cochran, A. (1985) Ap. J. 289, 388.

Combi, M.R. (1980) Ap. J. 241, 830.

Combi, M.R., and A.H. Delsemme (1980a) Ap. J. 237, 633.

Combi, M.R., and A.H. Delsemme (1980b) Ap. J. 237, 641.

Cucchiaro, A., and D. Malaise (1982) Astron. Astrophys. 114, 102.

Delsemme, A.H. (1982) in Comets (ed. L. Wilkening), The University of Arizona Press, Tucson, AZ, pp. 85-130.

Delsemme, A.H., and M.R. Combi (1983) Ap. J. 271, 388.

Eddington, A.S. (1910) M. N. R. A. S. 79, 442.

Festou, M.C. (1981a) Astron. Astrophys. 95, 69.

Festou, M.C. (1981b) Astron. Astrophys. 96, 52.

Giguere, P.T., and W.F. Huebner (1978) Ap. J. 223, 638.

Haser, L. (1957) Bull. Acad. Roy. Soc. Belgique 43, 740.

Haser, L. (1966) Mem. Soc. Roy. Sci. Liege 12, series 5, 233.

Huebner, W.F. (1985) Private communication.

Huebner, W.F., and C.W. Carpenter (1979) Los Alamos Sci. Lab. Report LA-8085-MS.

Huebner, W.F., and J.J. Keady (1982) International Conference on Cometary Exploration, Hungarian Academy of Sciences.

Johnson, J.R., U. Fink and S.M. Larson (1984) Icarus 60, 351.

Keller, H.U., and R.R. Meier (1976) Astron. Astrophys. 52, 273.

Kitamura, Y., O. Ashihara and T. Yamamota (1985) Icarus 61, 278.

Lambert, D.L., and A.C. Danks (1983) Ap. J. 268, 428.

Marconi, M.L., and D.A. Mendis (1982) Ap. J. 260, 386.

Mumma, M.J., R. Cody and D. Schleicher (1978) Bull. AAS 10, 587 (abstract).

Newburn, R.L., and H. Spinrad (1984) A. J. 89, 289.

Schleicher, D. (1984) Ph.D. thesis, University of Maryland.

Schleicher, D.G., and M.F. A'Hearn (1982) Ap. J. 258, 864.

Schleicher, D.G., and M.F. A'Hearn (1983) Bull. AAS 15, 806.

Schloerb, F.P., and E. Gerard (1985) A. J. 90, 1117.

Singh, P.D., E.F. vanDieshoeck and A. Dalgarno (1983) Icarus 56 184.

Stief, L.J. (1972) Nature 237, 29.

Tatum, J.B., and M.J. Gillespie (1977) Astrophys. J. 218, 569.

van Dishoeck, E.F., and A. Dalgarno (1984) Icarus 59, 305.

Wallace, L.V., and F.D. Miller (1958) A. J. 63, 213.

Weissman, P.R., and H.H. Kieffer (1984) Preprint.

Whipple, F.L. and W.F. Huebner (1976) Am. Rev. Astron. Astrophys. 14, 143.